

# Measurement of Leakage Neutron Spectra from Advanced Blanket Materials and Structural Materials Induced by D-T Neutrons

Takashi Nishio, Tetsuo Kondo, Hiroyuki Takagi, Kokoro<sup>1)</sup>, Isao Murata, Akito Takahashi, Fujio Maekawa<sup>2)</sup>, Yujiro Ikeda<sup>2)</sup> and Hiroshi Takeuchi<sup>2)</sup>

<sup>1)</sup> Department of Physics, University of Mawlamyine

<sup>2)</sup> Japan Atomic Energy Research Institute.

*Department of Nuclear Engineering, Osaka University*

*Yamadaoka, 2-1, Suita, 565-0871, Japan*

e-mail: nishio@newjapan.nucl.eng.osaka-u.ac.jp

D-T neutron benchmark experiments for LiAlO<sub>2</sub>, Li<sub>2</sub>TiO<sub>3</sub>, Li<sub>2</sub>ZrO<sub>3</sub>, Cu and W have been conducted at FNS of JAERI to validate five nuclear data files. The former three are promising advanced breeder materials and the latter two are important structural materials in a fusion reactor. From the results, all the nuclear data files were confirmed to be fairly reliable with respect to the prediction of neutron spectrum in the use of Li<sub>2</sub>TiO<sub>3</sub> and Cu. For LiAlO<sub>2</sub> and W, some large discrepancies between the experimental and calculated data were observed. For Li<sub>2</sub>ZrO<sub>3</sub>, the C/E values became very large for all the nuclear data files.

## 1. Introduction

In a fusion reactor, blanket and structural materials are placed adjacent to the reactor core. Of course they must be kept their intactness during operation. In a fusion reactor design to predict their intactness accurately, it is very important to carry out the benchmark experiments and to analyze their results for candidate blanket and structural materials. In the present study, we focus on ceramic materials including lithium such as LiAlO<sub>2</sub>, Li<sub>2</sub>TiO<sub>3</sub> and Li<sub>2</sub>ZrO<sub>3</sub> and Cu and W as an important structural material. Especially, LiAlO<sub>2</sub>, Li<sub>2</sub>TiO<sub>3</sub> and Li<sub>2</sub>ZrO<sub>3</sub> are regarded as advanced solid breeder materials because of their inherent advantages such as chemical stability at high temperature, good tritium recovery characteristic and so on. However no integral experiments exist using these blanket materials until now.

In Japan Atomic Energy Research Institute (JAERI), a project started several years ago and is now progressing including various fusion integral benchmark experiments [1]~[4]. The present benchmark study is a part of the project and has been undertaken under the collaboration of JAERI and Osaka University.

In the present study, leakage neutron spectra from LiAlO<sub>2</sub>, Li<sub>2</sub>TiO<sub>3</sub>, Li<sub>2</sub>ZrO<sub>3</sub>, Cu, and W assemblies have been measured and the analysis of the measured spectra has been carried out to validate accuracy of evaluated nuclear data files.

## 2. Experiment

The experiments were carried out at Fusion Neutronics Source (FNS) of JAERI. Table 1 shows the shape and thickness of used sample assemblies. Leakage neutron spectra from the sample assemblies

Table1 Sample assembly description

Sample	Shape*1	Dimensions (cm)
LiAlO <sub>2</sub>	Slab	25.4 x 25.4 x '10.2, '25.4
Li <sub>2</sub> TiO <sub>3</sub>	Slab	25.4 x 25.4 x '10.2, '25.4
Li <sub>2</sub> ZrO <sub>3</sub>	Pseudo-cylinder	47.6 φ **2 x '10.2, '25.4, '40.6
Cu	Slab	45.7 x 45.7 x '10.2, '25.4, '40.6
W	Slab	35.6 x 35.6 x '10.2, '20.3, '30.5

\*1 Sample are made by piling up unit bricks, the size of which is 5.08 x 5.08 x 5.08 cm<sup>3</sup>.

\*\*2 Equivalent diameter to conserve the front surface area.

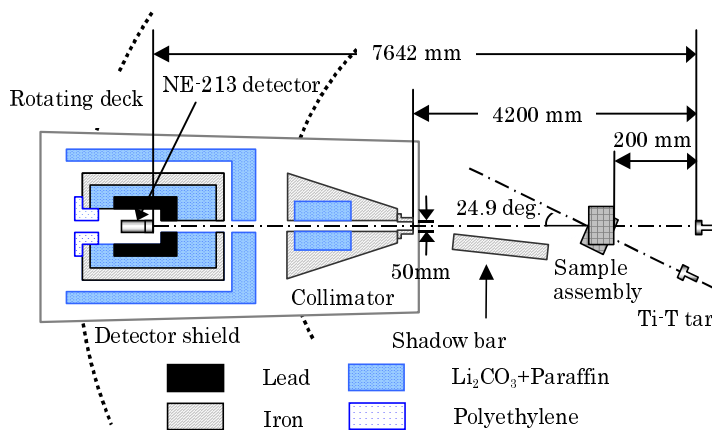


Fig.1 Cross-sectional view of the experimental arrangement

were measured using an NE-213 (2"-diam by 2"-long) scintillation detector by the time of flight (TOF) method for two emission angles of 0 and 24.9 degs. Fig.1 shows the experimental arrangement. A high energy-resolution measurement ranging from 0.05 to 15 MeV was successfully achieved by adoption of a long flight path as well as the pulse-shape-discrimination technique with three delay-line amplifiers, which were set to different gains. The block diagram of measuring system is shown in

Fig.2.

The detector efficiency was determined through three measurements to cover a wide energy dynamic range of the detector: (1) leakage neutron spectrum from a beryllium slab for lower energy, (2) Energy and angle differential elastic scattering cross section of hydrogen using a polyethylene sample for several to 13 MeV and (3) neutron source spectrum for 14 MeV. The fitted curve with these experimental results was used for data reduction of the measurements. Fig.3 shows the efficiency curve.

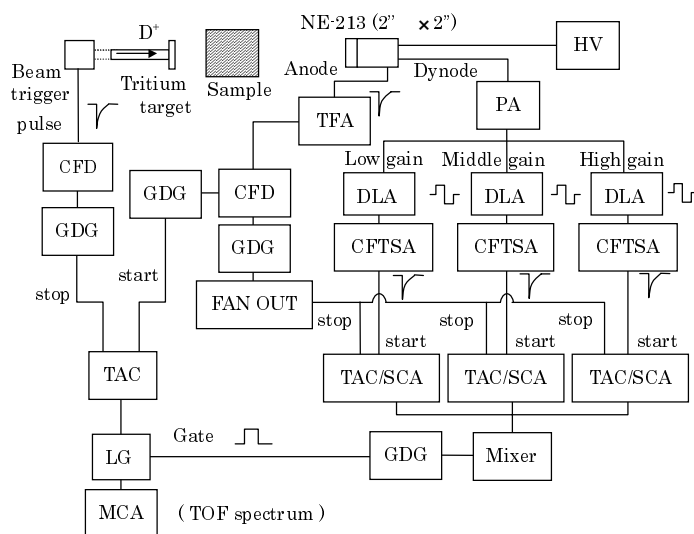
### 3. Data analysis

Analyses of the experiments were carried out with the three-dimensional Monte Carlo code MCNP-4B. For validation of cross section data, five evaluated nuclear data files, i.e., JENDL-3.2, JENDL-FF, ENDF/B-VI, FENDL/E-1.0, and FENDL/E-2.0 were selected as the cross section libraries listed in Table 2. The assemblies as well as the detector collimator were modeled precisely for the MCNP calculation. The measured source neutron spectrum was used as the neutron source in the calculation.

### 4. Results

#### i) LiAlO<sub>2</sub>

Figures 4 and 5 show the measured leakage neutron spectra for LiAlO<sub>2</sub> of 25.4 cm in thickness and scattering angle of 24.9 deg., and the C/E values, respectively. The calculated spectra are in fairly good agreement with the experimental data. However, an opposite trend is seen at the elastic peak, that is overestimation for 0 deg. and underestimation for 24.9 deg.



HV: High Voltage Power Supply  
 PA: Pre-Amplifier  
 TFA: Timing Filter Amplifier  
 DLA: Delay Line Amplifier  
 CFD: Constant Fraction Discriminator  
 CFTSCA: Constant Fraction Timing Single Channel Analyser  
 TAC/SCA: Time to Amplitude Converter  
 GDG: Gate and Delay Generator  
 TAC: Time to Amplitude Converter  
 LG: Linear Gate  
 MCA: Multi Channel Analyser

Fig.2 Block diagram of the measuring system

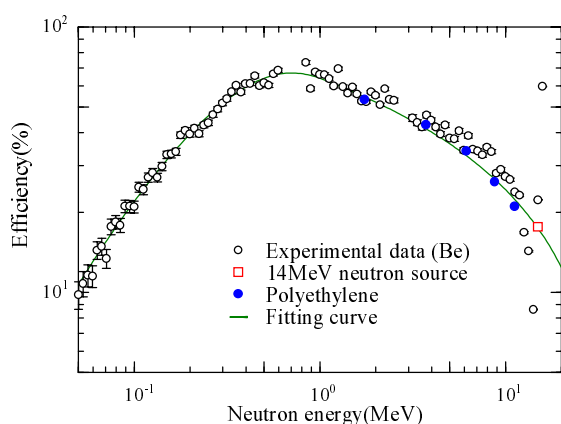


Fig.3 Measured efficiency of the NE-213 detector

experiment and calculation for the whole energy range and for all nuclear data files. However, the spectrum calculated with ENDF/B-VI is smaller than other calculations. This is understood from the neutron emission DDX comparison in Fig.9.

A valley around 10 MeV is observed similar to  $\text{LiAlO}_2$  in the calculated spectrum for only 24.9 deg. The valley might be caused by the discrepancy around about 10MeV of the neutron emission DDX for Ti as is shown in Fig.9. However Li or O might cause it, because this is also observed in  $\text{LiAlO}_2$ .

iii)  $\text{Li}_2\text{ZrO}_3$

Figures 10 and 11 show the measured leakage neutron spectra for  $\text{Li}_2\text{ZrO}_3$  of 25.4 cm in thickness and scattering angle of 24.9 deg., and the C/E values, respectively. The discrepancy between the experimental and calculated spectra is very large, that is overestimation of the calculation. This discrepancy is observed in all the other results, i.e., the more the thickness of assembly increases, the larger the discrepancy becomes. From the neutron emission DDX comparison as is shown in Fig.12., one can understand the difference among the calculated spectra below 1MeV, also in the C/E spectra. Similarly it is understood that the structures of spectra calculated with ENDF/B-VI were different from those of other nuclear data files.

iv) Cu

Figures 13 and 14 show the measured leakage neutron spectra for Cu of 10.16 cm in thickness and scattering angle of 24.9 deg., and the C/E values, respectively. The calculated spectra are in fairly good agreement with the experimental data. However, the elastic scattering peaks for 0 deg, do not agree with the calculations.

ENDF/B-VI and FENDL/E-2.0 are in excellent agreement with the experimental data

among five nuclear data files as one can see it from the comparison of the neutron emission DDX as is shown in Fig.15. The others show underestimation around 7 MeV.

v) W

Figures 16 and 17 show the measured leakage neutron spectra for W of 20.32 cm in thickness and scattering angle of 0 deg., and the C/E values, respectively. Some significant discrepancies between the experimental and calculated spectra are observed. From the

Table 2 Nuclear data files used in the calculation

Library name used in the present paper	Nuclear data quoted*1						
	Li	O	Al	Ti	Zr	Cu	W
JENDL-3.2	J32	J32	J32	J32	J32	J32	J32
JENDL-FF	J32	J32	JFF	JFF	JFF	JFF	JFF
ENDF/B-VI	B-VI	B-VI	B-VI	B-VI	B-VI	B-VI	BVI
FENDL/E-1.0	B-VI	B-VI	J31	J31	B2	B-VI	B-VI
FENDL/E-2.0	B-VI	J32	EF3	J31	JFF	B-VI	JFF

\*1 J32, JFF, B-VI, J31, EF3 and B2 are abbreviations of JENDL-3.2, JENDL-FF, ENDF/B-VI, JENDL-3.1, EFF-3 and BROND2, respectively.

comparison of the neutron emission DDX as is shown in Fig.18, one can understand the overestimation around 3 MeV for JENDL-FF and FENDL/E-2.0 and the underestimation around 10 MeV for ENDF/B-VI and FENDL/E-1.0.

As a whole, ENDF/B-VI and FENDL/E-1.0 are mostly reliable from the present measurement, though they show a little underestimation around 10 MeV from the DDX comparison.

### 5. Conclusion

D-T neutron benchmark experiments for advanced breeder materials and structural materials have been conducted to validate five nuclear data files. From the result, all the nuclear data files were confirmed to be fairly reliable with respect to the prediction of neutron spectrum in the use of  $\text{Li}_2\text{TiO}_3$  and Cu. For  $\text{LiAlO}_2$  and W, some large discrepancies between the experimental and calculated data were observed. For  $\text{Li}_2\text{ZrO}_3$ , the C/E values became very large for all the nuclear data files.

### Reference:

- [1] Kokoo, et al., Fusion Technol., 34, 980 (1998).
- [2] Maekawa F., et al., Fusion Technol., 34, 1018 (1998).
- [3] Maekawa F., et al., J. Nucl. Sci. Technol., (1998).
- [4] Murata I., et al., " Benchmark Experiment on  $\text{LiAlO}_2$ ,  $\text{Li}_2\text{TiO}_3$  and  $\text{Li}_2\text{ZrO}_3$  Assemblies with D-T Neutrons - Leakage Neutron Spectrum Measurement - " Proc. 5th Int. Symp. on Fusion Nucl. Technol., Roma, Sept. 19~24 (1999) to be published.
- [5] Takahashi A., et al., OKTAVIAN Report, A-92-01 (1992).

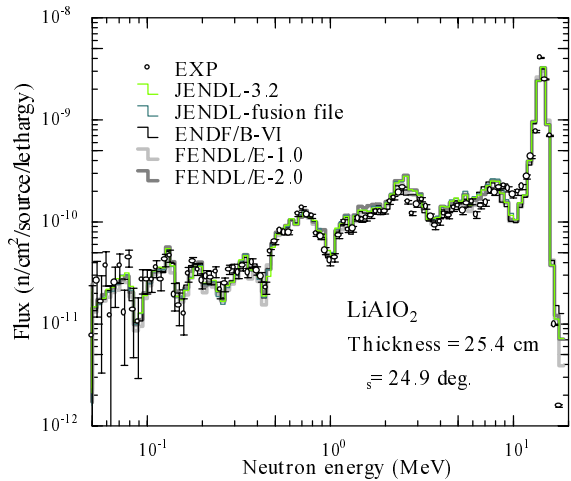


Fig.4 Neutron flux for  $\text{LiAlO}_2$  of 25.4 cm<sup>t</sup> at 24.9 deg.

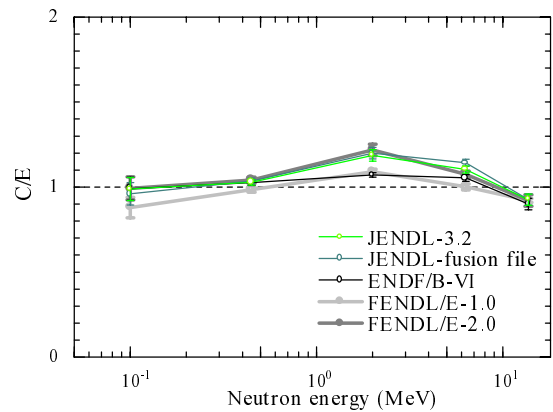


Fig.5 C/E for  $\text{LiAlO}_2$  of 25.4 cm<sup>t</sup> at 24.9 deg.

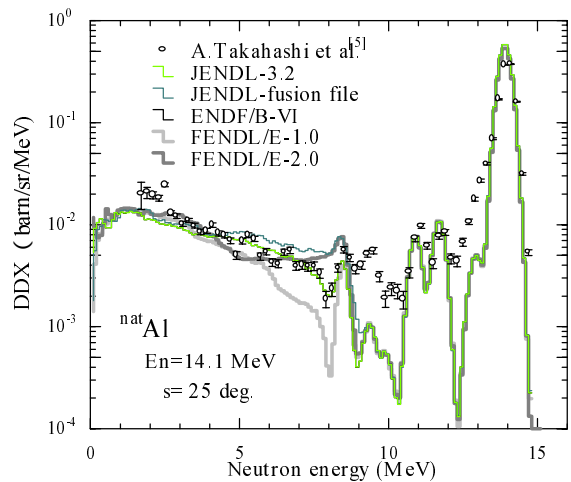


Fig.6 Evaluated neutron emission DDX of  $^{nat}\text{Al}$  at 25 deg. compared with the experimental data.

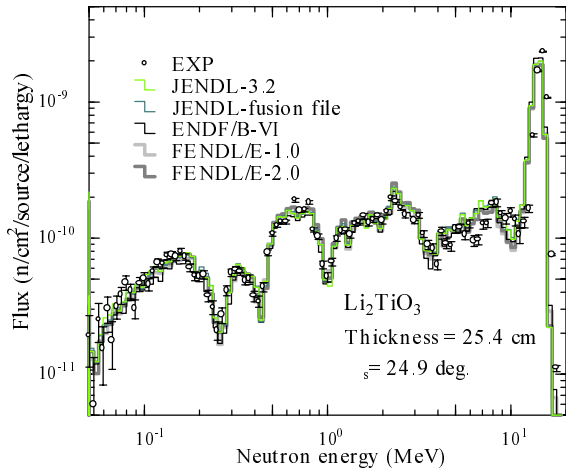


Fig.7 Neutron flux for  $\text{Li}_2\text{TiO}_3$  of  $25.4 \text{ cm}^2$  at  $24.9 \text{ deg}$ .

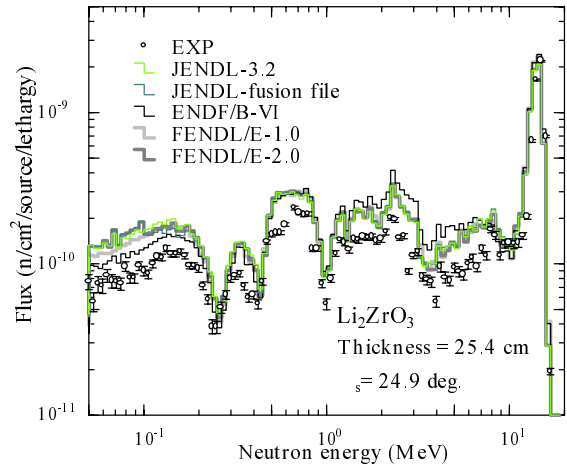


Fig.10 Neutron flux for  $\text{Li}_2\text{ZrO}_3$  of  $25.4 \text{ cm}^2$  at  $24.9 \text{ deg}$ .

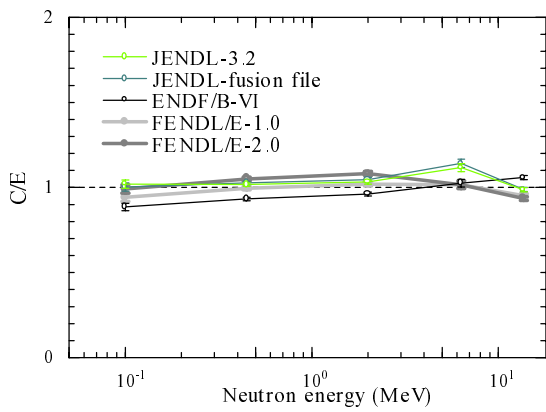


Fig.8 C/E for  $\text{Li}_2\text{TiO}_3$  of  $25.4 \text{ cm}^2$  at  $24.9 \text{ deg}$ .

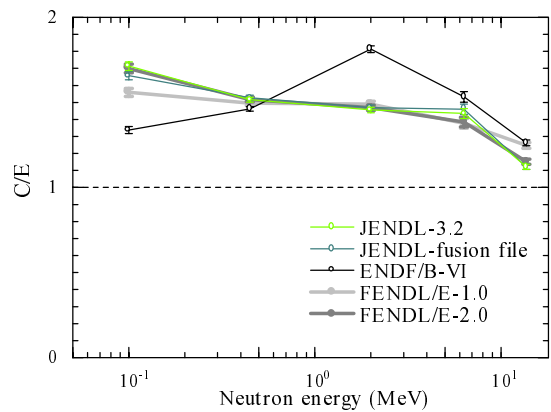


Fig.11 C/E for  $\text{Li}_2\text{ZrO}_3$  of  $25.4 \text{ cm}^2$  at  $24.9 \text{ deg}$ .

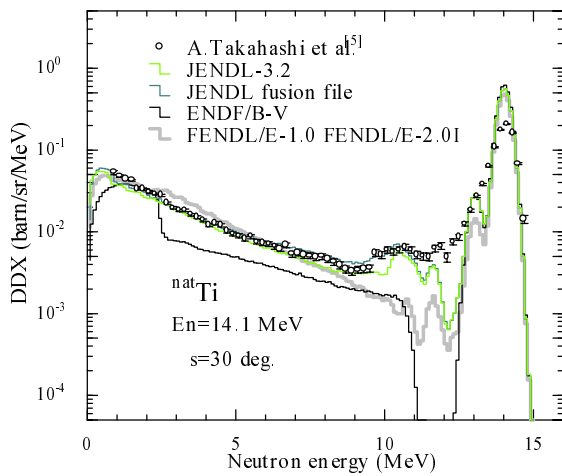


Fig.9 Evaluated neutron emission DDX of  $^{\text{nat}}\text{Ti}$  at  $30 \text{ deg}$  compared with the experimental data.

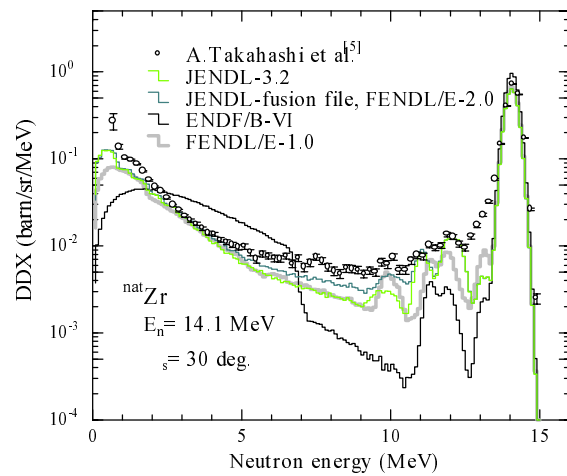


Fig.12 Evaluated neutron emission DDX of  $^{\text{nat}}\text{Zr}$  at  $30 \text{ deg}$  compared with the experimental data.

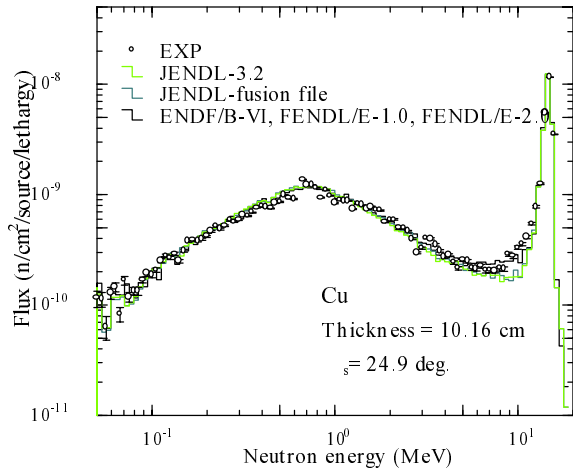


Fig.13 Neutron flux for Cu of 10.16 cm<sup>t</sup> at 24.9 deg.

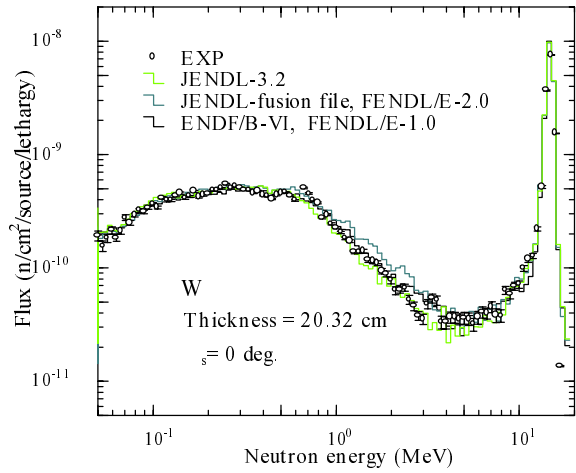


Fig.16 Neutron flux for W of 20.32 cm<sup>t</sup> at 0 deg.

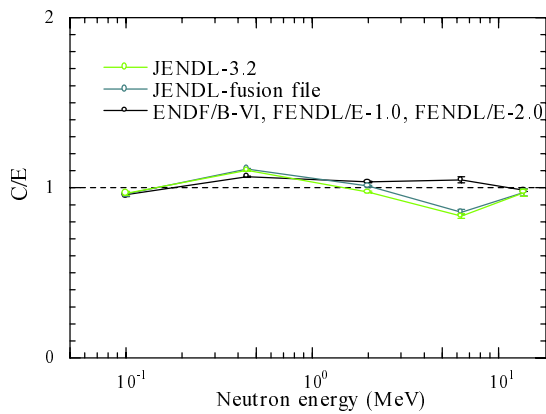


Fig.14 C/E for Cu of 10.16 cm<sup>t</sup> at 24.9 deg.

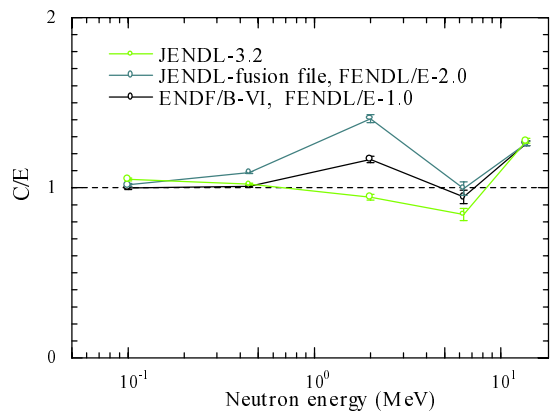


Fig.17 C/E for W of 20.32 cm<sup>t</sup> at 0 deg.

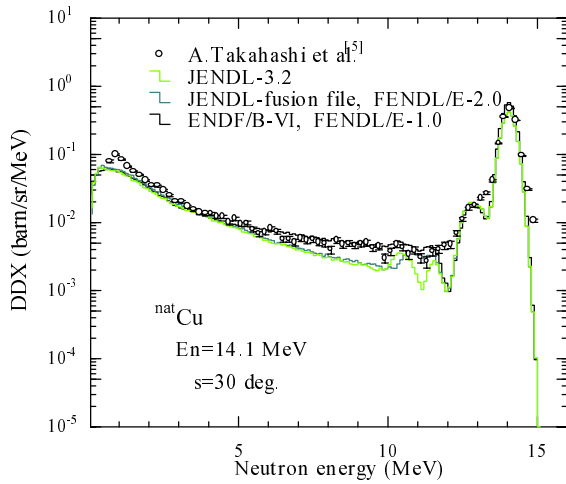


Fig.15 Evaluated neutron emission DDX of <sup>nat</sup>Cu at 30 deg. compared with the experimental data.

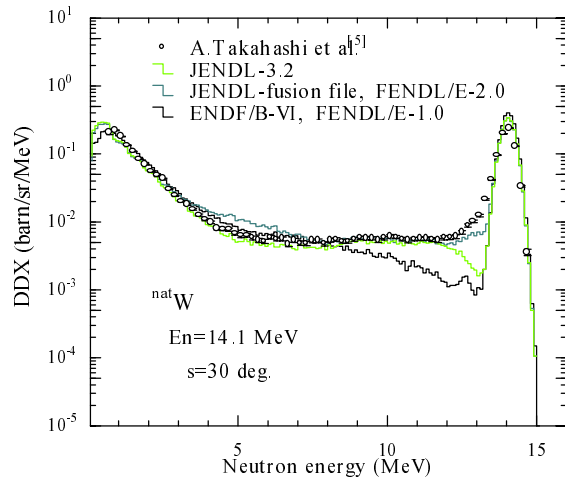


Fig.18 Evaluated neutron emission DDX of <sup>nat</sup>W at 30 deg. compared with the experimental data.